ChemComm

Chemical Communications

Accepted Manuscript

Volume 54
Number 1
4 January 2018
Pages 1-112

ChemComm

Chemical Communications

rsc.li/chemcomm

ISSN 1359-7345

ROYAL SOCIETY OF CHEMISTRY

COMMUNICATION
S. J. Connon, M. O. Senge et al
Conformational control of nonplanar free base porphyrins: towards bifunctional catalysts of tunable basicity

ROYAL SOCIETY OF CHEMISTRY

rsc.li/chemcomm

COMMUNICATION

Efficient photocatalytic CH$_4$ conversion into ethanol with O$_2$ over nitrogen vacancy-rich carbon nitride at room temperature

Zhongshan Yang,[ab] Qiqi Zhang,[ab] Liteng Ren,[ab] Xin Chen,[ab] Defa Wang,[ab] Lequan Liu,*[ab] and Jinhua Ye [abc]

A record ethanol production rate of 281.6 μmol g^{-1} h^{-1} was achieved in photocatalytic methane conversion over nitrogen vacancy-rich carbon nitride at room temperature. Systematic studies demonstrate CH$_4$ was activated by highly active ·OH radical generated from O$_2$ photo-reduction with H$_2$O via H$_2$O$_2$.

Methane, as an abundant resource on earth and an important feedstock for chemicals, its efficient conversion has been attracting great attentions.[1] Due to highly stable regular tetrahedron structure, traditional indirect transformation of methane, or syngas route, bears tremendous energy input.[2] It is highly desirable to develop efficient route to transform methane into up-market products under mild conditions. Photocatalysis, as a burgeoning technology which could fulfil water splitting and environmental remediation at room temperatures, brings this field new perspectives and feasibility.[3-6] WO$_3$,[7-9] TiO$_2$,[10, 11] and g-C$_3$N$_4$[12-14] have been reported for photocatalytic conversion of methane into methanol, formic acid and methyl hydroperoxide so on. However, it still faces great challenge to promote the efficiencies, particular for value-added and more attractive products like ethanol.

The selection of oxidant plays a crucial role in efficient photocatalytic conversion of methane into oxygenates.[15] Among them, water is theoretically an ideal oxidant but suffers from rather low conversion efficiencies.[16-18] Hydrogen peroxide is a strong and clean oxidant, while its high cost and difficulties in transportation or storage restrict its application.[19] From the perspective of availability and operating safety, oxygen is an attractive candidate for efficient photocatalytic conversion of methane into oxygenates. A recent work reported by Ye et, al. primarily validates its feasibility.[20] While

CH$_4$ was mainly photochemically converted into CH$_3$OOH, and the ·OOH radicals were identified as the active species. As ·OH possesses higher oxidative potential,[20] it is promising that ·OH radicals generated from oxygen reduction can be utilized for efficient methane activation. Fan et al. made an attempt and reported that methane was activated by ·OH radicals in photocatalytic conversion of methane into oxygenates.[21] Nevertheless, ·OH radicals were mainly generated from H$_2$O oxidation rather than from O$_2$ reduction. It is highly desirable to develop efficient system for transforming CH$_4$ into ethanol with O$_2$ under mild conditions.

In this work, highly efficient photocatalytic conversion of CH$_4$ into ethanol was achieved over the nitrogen vacancy (V$_N$) -rich carbon nitride with O$_2$ as oxidant. Systematic study indicated that methane molecules were activated by ·OH radicals photo-generated from O$_2$ reduction with H$_2$O via H$_2$O$_2$. Moreover, the introduction of V$_N$ enhanced the light absorption and charge carrier separation efficiency, then promoted the production of H$_2$O$_2$, which ultimately facilitated the photocatalytic conversion of methane into ethanol.

Pristine g-C$_3$N$_4$ (CN) was synthesized through a thermal polymerization method by using melamine as the precursor. The reduced carbon nitride samples (RCN-x) with nitrogen vacancy were synthesized by a modified solid-state chemical reduction method (x = 3, 5, 7, represent the weight ratio of CN:NaBH$_4$ were 1:3, 1:5, 1:7) with the purpose of efficient photocatalytic O$_2$ reduction to oxidative radicals.[22] Morphology and microstructure of the as-synthesized samples were characterized by scanning electron microscopy (SEM) and transmission electron microscopy (TEM) (Fig. 1a-b, Fig. S1). Compared to CN sample，the RCN sample is fluffy and the surface is more rough and uneven. Many edges and notches were formed, which may increase the reactive areas and provide more active sites for oxygen reduction.[23] The crystal structures of CN and RCN samples were shown in the Fig. S2. Subsequently, series of characterizations were executed to verify the formation of nitrogen vacancies in RCN samples. As demonstrated in Fig. 1c, RCN samples exhibited obvious electron spin resonance (ESR) signals with g value of 2.002, which could be attributed to unpaired electrons on the carbon atoms of the heptazine rings due to the formation of V$_N$.[5] It finds further support from Fourier transform infrared spectroscopy (FT-IR) spectra, where

[a] *TJU-NIMS International Collaboration Laboratory, Key Laboratory of Advanced Ceramics and Machining Technology (Ministry of Education) and Tianjin Key Laboratory of Composite and Functional Materials, School of Material Science and Engineering, Tianjin University, Tianjin 300072, China.*
E-mail: Lequan.Liu@tju.edu.cn.
[b] *Collaborative Innovation Centre of Chemical Science and Engineering (Tianjin), Tianjin 300072, China*
[c] *International Centre for Materials Nanoarchitectonics (WPI-MANA), National Institute for Materials Science (NIMS), Japan.*
† Electronic Supplementary Information (ESI) available.
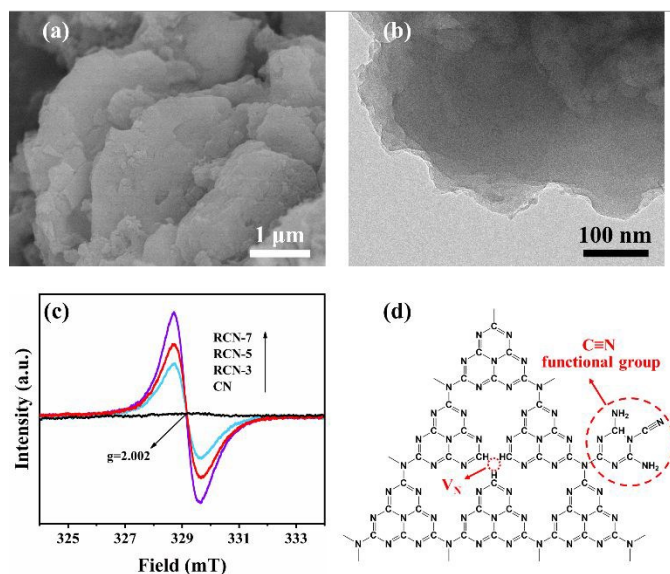See DOI: 10.1039/x0xx00000x

ChemComm Accepted Manuscript

Fig. 1 (a) SEM and (b) TEM image for RCN. (c) ESR spectra of CN and RCN samples. (d) Graphic illustration of formed V_N and C≡N groups in RCN samples.

a new vibration bonds emerged at 2180 cm^{-1} showing the formation of C≡N functional groups in RCN samples (Fig. S3). Furthermore, an enhancement of the ESR signal intensity was observed along with the increase of CN/NaBH$_4$ ratio, indicating the growing concentration of nitrogen vacancy. Similar trends also manifested in the decreased C-N=C/N-(C)$_3$ ratio from X-ray photoelectron spectroscopy (XPS) analysis (Fig. S4). Moreover, the decreased C-N=C/N-(C)$_3$ ratio of CN (2.68) and RCN (1.93) samples from N 1s XPS spectra indicates that the V_N are majorly at C-N=C sites.[5] The graphic illustration of formed V_N and C≡N functional groups are shown in the Fig. 1d.

The photocatalytic methane conversion reaction was performed at room temperature (25 ± 1 ℃) under the pressure of 0.1 MPa O$_2$ (purity, 99.99%) and 2 MPa CH$_4$ (purity, 99.999%) in a 50 mL stainless-steel autoclave equipped with a quartz window to allow light irradiation (Fig. S5). A 300 W Xe lamp was employed as the light source, the light intensity was determined to be 100 mW cm^{-2} (Fig. S6). The generated products in liquid and gas phase were quantified by ^{1}H nuclear magnetic resonance (NMR) and gas chromatography (GC) measurements, respectively (Fig. S7, Fig. S8). After the amount of catalyst was optimized to 20 mg (Fig. S9), blank experiments were carried out, and they revealed the indispensable role of oxygen and light in the photocatalytic conversion of methane (Fig. S10). Subsequently, as shown in Fig. 2a, photocatalytic conversion of methane into oxygenates occurred over CN sample, though the conversion rate was relatively low. Impressively, an C$_2$H$_5$OH production rate of 211.2 μmol g^{-1} h^{-1} with a selectivity of 74.1% was achieved over RCN-5. These results indicate nitrogen vacancies in g-C$_3$N$_4$ remarkably promote photocatalytic methane conversion into ethanol with O$_2$. Moreover, the nitrogen vacancy played an important role in enhanced alcohols' selectivity as demonstrated in a control experiment under dark conditions (Fig. S11). As the concentration of possible H$_2$O$_2$ or ·OH oxidative intermediate varied with light irradiation, the ethanol production rate as a function of
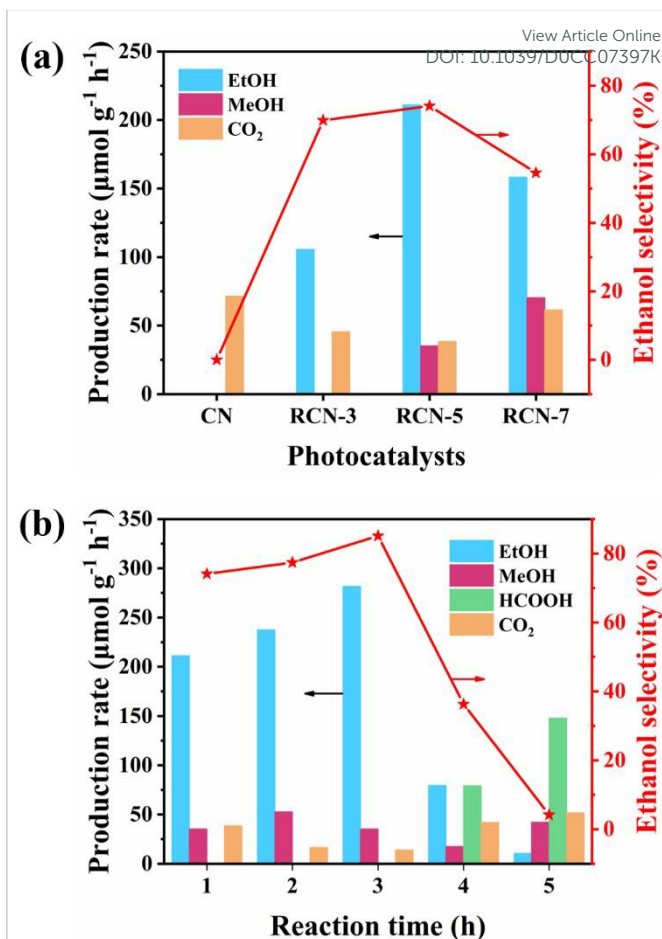
Fig. 2 (a) Photocatalytic conversion of methane over CN and RCN-x samples in 1 h. (b) Average production rate of photocatalytic methane conversion over RCN-5 during different reaction time (1 h, 2 h, 3 h, 4 h, 5 h).

reaction time was investigated (Fig. 2b). An average ethanol production rate in 3 hours reached as high as 281.6 μmol g^{-1} h^{-1} over RCN-5. To the best of our knowledge, it is a new record for C$_2$H$_5$OH product among all the photocatalytic methane conversion reaction reported under room temperatures (Table S1). Moreover, the photocatalysts after reaction remains relatively stable known from XRD pattern and TEM images in the Fig S12-13. As the reaction time was prolonged to 4 hours or 5 hours, the C$_2$H$_5$OH production rate decreased accompanied with the HCOOH and CO$_2$ production rate increased. This result may indicate the overoxidation of produced alcohols, which will be discussed later.

To clarify the oxidative intermediates during the photocatalytic CH$_4$ conversion, H$_2$O$_2$ production over CN and RCN-x samples was first studied (Fig. 3a, left). As can be seen, H$_2$O$_2$ was detected over all samples, with C/N atomic ratio ranging from 0.63 to 0.75 as determined by Elemental Analysis (EA) (Table S2). According to previous work, the production of H$_2$O$_2$ was mainly generated by two-electron reduction of O$_2$ over reduced g-C$_3$N$_4$.[22] Moreover, H$_2$O$_2$ production rate was obviously accelerated along with the increase of C/N atomic ratio. Similar trend was observed by XPS analysis (Table S3). These results agree well with the performance of photocatalytic CH$_4$ conversion into ethanol, suggesting the route of photo-reduction of O$_2$ to H$_2$O$_2$. The generation of ·OH radicals was clarified by ESR

measurement and photoluminescence (PL) spectra. As shown in Figure 3b, the four-peak signature with a 1:2:2:1 line shape in the ESR spectra is ascribed to the presence of ·OH radicals.[4] As the valence band (VB) of g-C_3N_4 is unable to oxidize H_2O to form ·OH radicals (E(H_2O/·OH)=2.8 V vs. RHE, pH=7).[13] Furthermore，a much higher ESR signal of RCN-5 was detected as compared to CN, indicating V_N remarkably enhanced the generation of ·OH radicals. Similar trend was further confirmed in the PL test using coumarin as a probe

molecule (Fig. S14).[24] In order to further identify the role played by ·OH radicals, a control experiment using tert-butanol (TBA) as the trapping agent was carried out (Fig. 3a, right). After capturing the ·OH radicals, no obvious ethanol was detected. These results revealed that ·OH radicals were directly involved in photocatalytic CH_4 conversion into ethanol over RCN-5. It is reasonable to draw a conclusion that highly active ·OH radicals, mainly generated from photo-reduction of O_2 with H_2O via H_2O_2, activate and transform methane molecules into ethanol. Based on the discussions above, the proposed reaction route of photocatalytic methane conversion with oxygen in water over RCN was illustrated in Fig. 3c.

It is worthy to point out that the concentration of generated H_2O_2 is an important factor influencing the performance of photocatalytic methane conversion.[11, 25] As demonstrated in Fig. 2a, the ethanol production over RCN-7 decreased accompanied with increased CO_2 production as compared with RCN-5, though the H_2O_2 production was further accelerated. This could be ascribed to the overoxidation of produced alcohols by excessive ·OH radicals.[11, 18] Similar phenomenon was also observed in Fig 2b and Fig. S15. That is the concentration of in-situ generated H_2O_2 therefore exists an optimal value,[14] which was determined to be 217.1 µmol L^{-1} in this work.

UV-vis diffuse reflectance spectroscopy (UV-vis DRS), PL characterization and electrochemical impedance spectroscopy (EIS) measurement were adopted to study the intrinsic characteristics of photocatalysts. Compared with CN, RCN-5 exhibited a red shift of the absorption edge, depicting the enhancement of light absorption in both UV region and visible region (Fig. 4a). The extended light absorption could be attributed to the incorporation of C≡N group.[26] In addition, as shown in the inset, the results revealed a narrower bandgap of the RCN-5 sample (2.65 eV) compared to CN (2.81 eV) due to the introduction of nitrogen vacancy.[22] In other words, the introduction of nitrogen vacancy broadened light absorption and narrowed the bandgap. The fluorescence decays (Fig. 4b) fitted with three exponential types (Table S4) demonstrated that RCN-5 possesses a much shorter fluorescence lifetime (4.38 ns) than CN (10.18 ns), indicating that the charge carrier separation efficiency was greatly improved.[27, 28] A much lower steady state PL intensity was observed, which further verified the enhanced charge carrier separation efficiency (Fig. S16). This might be caused by alleviation of charge carrier recombination due to conduction band (CB)-to-defect states charge transfer.[29, 30] The EIS pattern displays that RCN-5 has a smaller arc radius than CN, showing a lower charge transfer resistance (Fig. S17), indicating that the photogenerated electrons and holes could transfer to the interface and be consumed by the surface reaction quickly.[31] Thus, more efficient electron can localize on the surface terminal sites of RCN samples, which promoted the photocatalytic reduction of O_2.[32]

In summary, efficient photocatalytic conversion of CH_4 with an ethanol production rate of 281.6 µmol g^{-1} h^{-1} was determined over RCN-5 at room temperature. Moreover, systematic investigations and characterizations indicated that methane molecules were activated by ·OH radicals generated from O_2 reduction through H_2O_2. The highly active ·OH radicals activate and transform CH_4 into ethanol. The introduction of nitrogen vacancy enhanced the light absorption and improved the charge carrier separation efficiency, then promoted the H_2O_2 production through oxygen reduction with water, which ultimately boosted the efficient photocatalytic
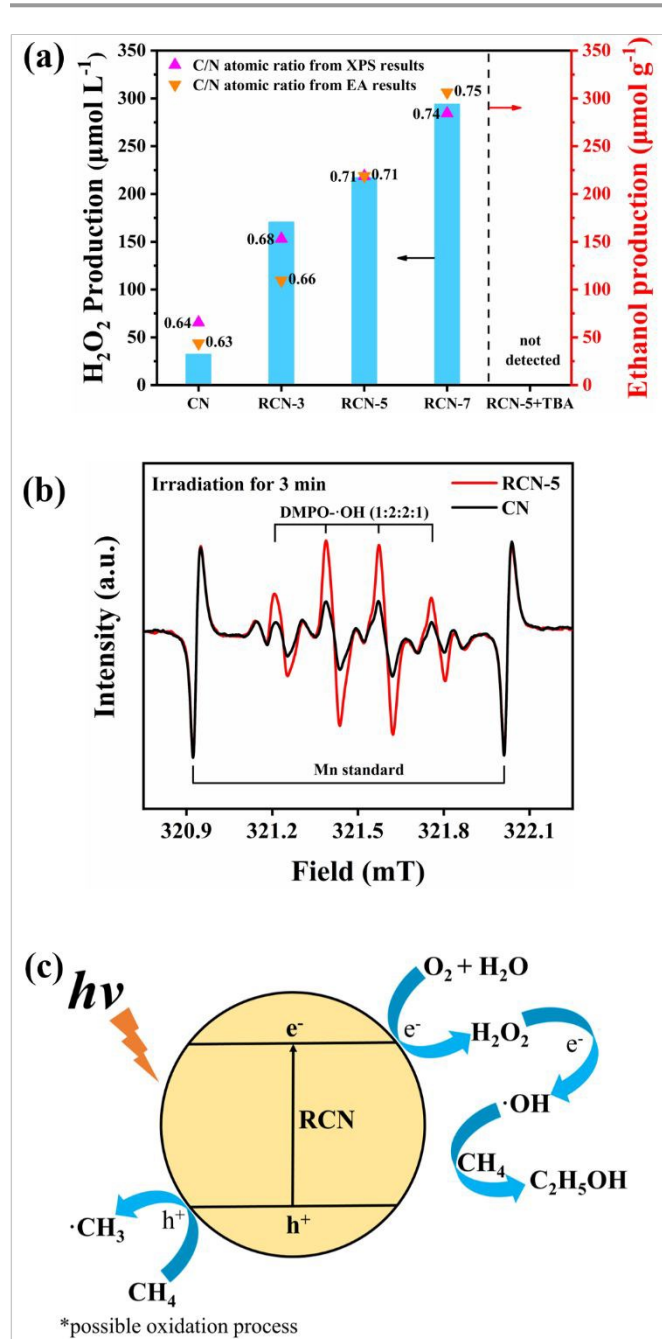
Fig. 3 (a) Photocatalytic H_2O_2 production over CN and RCN-x with different content of nitrogen vacancies in 3 hours (▲ and ▼ represents the C/N atomic ratio from XPS analysis and EA results, respectively). The right is a control experiment using tert-butanol (TBA) as the trapping agent for ·OH radicals. (b) ESR spectra of CN and RCN-5 with 5, 5-dimethyl-1-pyrroline N-oxide (DMPO) as a trapping agent. (c) The hypothesized reaction route of photocatalytic methane conversion with Oxygen in water over RCN.
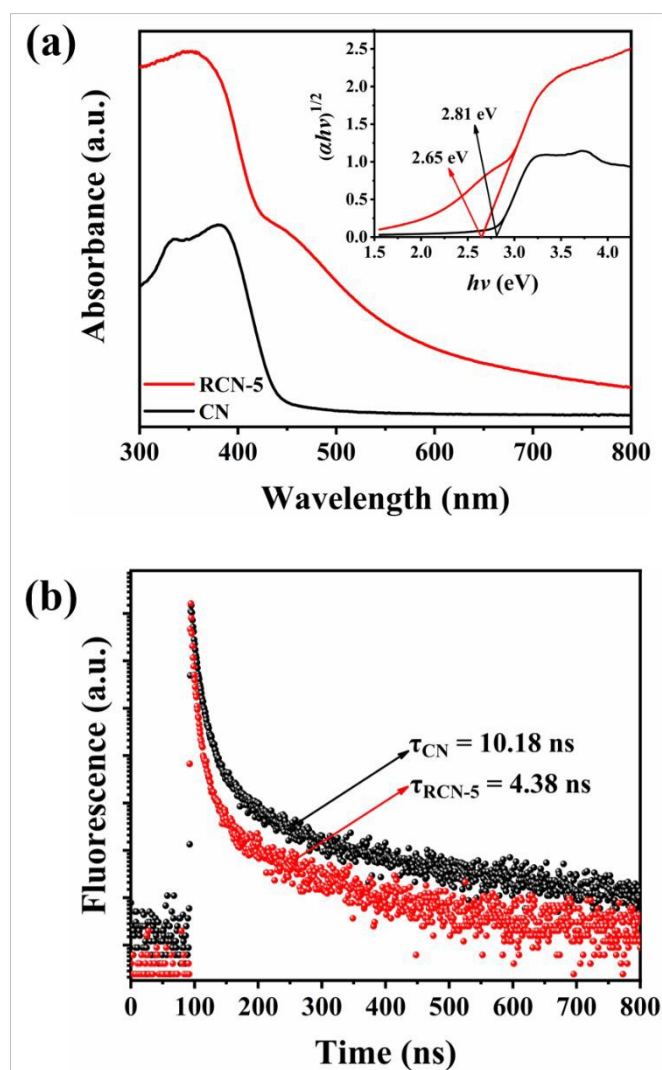
Fig. 4 (a) UV-vis DRS spectra and transformed Kubelka-Munk function versus photon energy plots (inset) of CN and RCN. (b) Fluorescence decays of CN and RCN-5.

methane conversion into ethanol. The discovery reported may provide a novel and feasible route to promote the efficiency of photocatalytic methane conversion.

Conflicts of interest

There are no conflicts to declare.

References

1   X. Meng, X. Cui, N. P. Rajan, L. Yu, D. Deng and X. Bao, *Chem*, 2019, **5**, 2296-2325.
2   H. Song, X. Meng, Z.-j. Wang, H. Liu and J. Ye, *Joule*, 2019, **3**, 1606-1636.
3   Z. Jiang, L. Wang, J. Lei, Y. Liu and J. Zhang, *Appl. Catal., B*, 2019, **241**, 367-374.
4   Y. Li, S. Ouyang, H. Xu, X. Wang, Y. Bi, Y. Zhang and J. Ye, *J. Am. Chem. Soc.*, 2016, **138**, 13289-13297.
5   Y. Xiao, G. Tian, W. Li, Y. Xie, B. Jiang, C. Tian, D. Zhao and H. Fu, *J. Am. Chem. Soc.*, 2019, **141**, 2508-2515.
6   Z. Zou, J. Ye, K. Sayama and H. Arakawa, *Nature*, 2001, **414**, 625-627.
7   M. A. Gondal, A. Hameed and A. Suwaiyan, *Appl. Catal., A*, 2003, **243**, 165-174.
8   K. Villa, S. Murcia-López, J. R. Morante and T. Andreu, *Appl. Catal., B*, 2016, **187**, 30-36.
9   J. Yang, J. Hao, J. Wei, J. Dai and Y. Li, *Fuel*, 2020, **266**, 117104.
10 Y. Zeng, H. Liu, J. Wang, X. Wu, S. Wang, *Catal. Sci. Technol.*, 2020, **10**, 2329-2332.
11 J. Xie, R. Jin, A. Li, Y. Bi, Q. Ruan, Y. Deng, Y. Zhang, S. Yao, G. Sankar, D. Ma and J. Tang, *Nat. Catal.*, 2018, **1**, 889-896.
12 Y. Li, J. Li, G. Zhang, K. Wang and X. Wu, *ACS Sustainable Chem. Eng.*, 2019, **7**, 4382-4389.
13 S. Shi, Z. Sun, C. Bao, T. Gao and Y. Hu, *Int. J. Energy Res.*, 2020, **44**, 2740-2753.
14 Y. Zhou, L. Zhang and W. Wang, *Nat. Commun.*, 2019, **10**, 506.
15 L. Yuliati and H. Yoshida, *Chem. Soc. Rev.*, 2008, **37**, 1592-1602.
16 S. Murcia-López, K. Villa, T. Andreu and J. R. Morante, *ACS Catal.*, 2014, **4**, 3013-3019.
17 H. Ito, R. Kondo, K. Yoshimori and T. Kamachi, *Chembiochem*, 2018, **19**, 2152-2155.
18 J. Du, W. Chen, G. Wu, Y. Song, X. Dong, G. Li, J. Fang, J. Wei, Y. Sun, Catalysts, 2020, **10**, 196.
19 Á. López-Martín, A. Caballero and G. Colón, *J. Photochem. Photobiol. A.*, 2017, **349**, 216-223.
20 H. Song, X. Meng, S. Wang, W. Zhou, X. Wang, T. Kako, J. Ye, *J. Am. Chem. Soc.*, 2019, **141**, 20507-20515.
21 W. Zhou, X. Qiu, Y. Jiang, Y. Fan, S. Wei, D. Han, L. Niu and Z. Tang, *J. Mater. Chem. A*, 2020, **8**, 13277-13284.
22 Z. Zhu, H. Pan, M. Murugananthan, J. Gong and Y. Zhang, *Appl. Catal., B*, 2018, **232**, 19-25.
23 J. Huang, S. Wen, G. Chen, W. Chen, G. Wang, H. Fan, D. Chen, C. Song, M. Li, X. Wang, L. Li, M. Tao, B. Li, X. Wang and K. Ostrikov, *Appl. Catal., B*, 2020, **277**, 119220.
24 Q. Xiang, J. Yu and P. K. Wong, *J. Colloid Interface Sci.*, 2011, **357**, 163-167.
25 X. Cui, H. Li, Y. Wang, Y. Hu, L. Hua, H. Li, X. Han, Q. Liu, F. Yang, L. He, X. Chen, Q. Li, J. Xiao, D. Deng and X. Bao, *Chem*, 2018, **4**, 1902-1910.
26 G. Liu, G. Zhao, W. Zhou, Y. Liu, H. Pang, H. Zhang, D. Hao, X. Meng, P. Li, T. Kako and J. Ye, *Adv. Funct. Mater.*, 2016, **26**, 6822-6829.
27 A. Fu, X. Chen, L. Tong, D. Wang, L. Liu and J. Ye, *ACS Appl. Mater. Interfaces,* 2019, **11**, 24154-24163.
28 T. Huang, S. Pan, L. Shi, A. Yu, X. Wang and Y. Fu, *Nanoscale*, 2020, **12**, 1833-1841.
29 M. Z. Rahman and C. B. Mullins, *Acc. Chem. Res.*, 2019, **52**, 248-257.
30 G. Ge, M. Liu, C. Liu, W. Zhou, D. Wang, L. Liu and J. Ye, *J. Mater. Chem. A*, 2019, **7**, 9222-9229.
31 L. Shi, L. Yang, W. Zhou, Y. Liu, L. Yin, X. Hai, H. Song and J. Ye, *Small*, 2018, **14**,1703142.
32 Y. Wang, D. Meng and X. Zhao, *Appl. Catal., B*, 2020, **273**,119064.
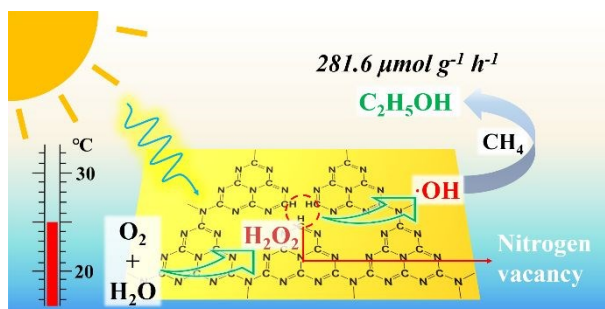
An ethanol production rate as high as 281.6 μmol g^{-1} h^{-1} was achieved during photocatalytic CH$_4$ conversion with O$_2$ at room temperature.